Colloid Polym Sci (2009) 287:569–575
DOI 10.1007/s00396-009-2004-5

ORIGINAL CONTRIBUTION

Adsorption behavior of organic halides on zeolites

Takae Kawai · Kazuo Tsutsumi

Received: 18 November 2008 / Accepted: 9 January 2009 / Published online: 6 February 2009

Abstract The adsorption behavior and the differential heat of adsorption of chloroform were measured on various types of zeolite (faujasite, ZSM-5 and mordenite) with different Si/Al ratios. The results reveal that saturated adsorption is almost proportional to the micropore volume and is independent of the micropore structure or the Si/Al ratio. However, initial heat of adsorption was the highest (90 kJ mol^{-1}) on the mordenite with low Si/Al ratio, while low on the faujasite with high Si/Al ratio or ZSM-5 (50 kJ mol^{-1}). Change in initial heat of adsorption with Si/Al ratio is small for faujasite or mordenite and large for ZSM-5. For the comparison, trichloroethylene adsorption behavior of zeolite was also investigated. Saturated adsorption of trichloroethylene was almost constant for all types of zeolite, while the faujasite with high Si/Al ratio exhibited an adsorption isotherm of type V in BDDT (Brunauer, Deming, Deming and Teller) classification. The tendencies of heat of immersion are similar to the results of the initial heat of adsorption.

Keywords Zeolite · Adsorption · Chloroform · Trichloroethylene · Heat of adsorption

T. Kawai (✉)
Department of Chemical and Biochemical Engineering,
Toyama National College of Technology,
13, Hongo-machi,
Toyama 939-8630, Japan
e-mail: kawai@toyama-nct.ac.jp

K. Tsutsumi
International Cooperation Center for Engineering Education
Development, Toyohashi University of Technology,
Tempaku-cho,
Toyohashi 441-8580, Japan
e-mail: tsutsumi@icceed.tut.ac.jp

Introduction

The current water purification process involves several cycles of chlorine treatment. Through this chlorine treatment, chlorination reaction occurs on humic acid and other organic substances in raw water, producing various organic halides. Among these, trihalomethanes (chloroform, bromodichloromethane, dibromochloromethane, and bromoform) are carcinogenic and must be removed. Various techniques have been studied to remove them, and those using adsorbents such as activated carbon [1–11] or activated carbon fiber [4, 12–16] have actively been studied and put into practical use. Techniques using the adsorptive feature of zeolites have also been reported recently [17–24].

Zeolite is crystalline adsorbent in which molecular-size micropores are arranged in an orderly manner. Since typical zeolite contains in its framework a large amount of aluminum molecules which serve as active sites, it is hydrophilic and in general cannot be used for water purification. The authors, therefore, prepared hydrophobic zeolites by various methods [25] and reported their characteristics of adsorbing various organic substances from water [26, 27]. As for trihalomethanes as well, we studied faujasite, ZSM-5 and mordenite with various Si/Al ratios regarding the behavior of adsorbing chloroform from aqueous solution [28, 29]. These studies revealed the relationship between the chloroform adsorption from aqueous solution and the Si/Al ratio, suggesting that the latter plays an important role for the hydrophile–hydrophobe balance of zeolite micropore surface. Zeolites with low Si/Al ratio (i.e., high Al content) are highly hydrophilic and therefore adsorb selectively water rather than chloroform from aqueous solution. On the other hand, zeolites with high Si/Al ratio (i.e., low Al content) are hydrophobic and adsorb a large amount of chloroform.

In the present study, in order to obtain detailed information about the interaction between chloroform molecules and zeolite micropore surface, differential heats of adsorption and heats of immersion of chloroform onto three types of zeolite (faujasite, ZSM-5, and mordenite) were calorimetrically determined, and effects of Si/Al ratio were evaluated. Trichloroethylene adsorption on faujasites with different Si/Al ratio was also measured for comparison with chloroform adsorption.

Experimental

Samples of three types of zeolites (faujasite, ZSM-5, and mordenite), which are different in framework structure and in Si/Al ratio, were used as adsorbents, the chemical composition of which is given in Table 1. Na-faujasite samples with various Si/Al ratios were prepared by treating Na-$Y_{5.5}$ (Toso) with hydrosulfuric acid/silicilic acid [30, 31] and $SiCl_4$ [32–34] for dealuminization. H-Y_{770} was a hydrothermal- and acid-treated sample (Toso) [35, 36]. Na-ZSM-5 samples with various Si/Al ratios were supplied from Mobil Catalysts of Japan. Na-Mordenite samples with various Si/Al ratios were supplied from Tosoh Corporation.

Water adsorption onto each faujasite sample was measured at a temperature of 303 K by the gravimetric method using quartz spring and a charge-coupled device. About 300 mg of adsorbent was placed in a specimen basket and pretreated for 5 h at 673 K under 1 mPa. Differential heats of adsorption of chloroform were measured at 303 K with a conduction calorimeter [37, 38] equipped with a volumetric adsorption system. About 500 mg of adsorbent placed in a cell was pretreated for 12 h at 673 K under 1 mPa. Before adsorption measurements, adsorbates were purified by the freeze–pump–thaw cycle.

Table 1 Chemical Compositions of the used samples

Sample	Type	Composition	Ref.
Na-$Y_{5.5}$	Faujasite	$Na_2O{\cdot}Al_2O_3{\cdot}(SiO_2)_{5.5}{\cdot}nH_2O$	[28]
Na-Y_{42}	Faujasite	$Na_2O{\cdot}Al_2O_3{\cdot}(SiO_2)_{42}{\cdot}nH_2O$	[28]
Na-Y_{130}	Faujasite	$Na_2O{\cdot}Al_2O_3{\cdot}(SiO_2)_{130}{\cdot}nH_2O$	[28]
Na-Y_{344}	Faujasite	$Na_2O{\cdot}Al_2O_3{\cdot}(SiO_2)_{344}{\cdot}nH_2O$	[28]
H-Y_{770}	Faujasite	$Al_2O_3{\cdot}(SiO_2)_{770}{\cdot}nH_2O$	[35, 36]
ZSM-5-25Na	ZSM-5	$Na_2O{\cdot}Al_2O_3{\cdot}(SiO_2)_{26}{\cdot}nH_2O$	[26]
ZSM-5-70Na	ZSM-5	$Na_2O{\cdot}Al_2O_3{\cdot}(SiO_2)_{94}{\cdot}nH_2O$	[26]
ZSM-5-1000Na	ZSM-5	$Na_2O{\cdot}Al_2O_3{\cdot}(SiO_2)_{1400}{\cdot}nH_2O$	[26]
M-10	Mordenite	$Na_2O{\cdot}Al_2O_3{\cdot}(SiO_2)_{9.8}{\cdot}nH_2O$	[28]
M-20	Mordenite	$Na_2O{\cdot}Al_2O_3{\cdot}(SiO_2)_{20}{\cdot}nH_2O$	[28]

Heats of immersion of zeolites into chloroform were measured at 298 K by use of a twin conduction-type calorimeter. The sample was evacuated at 673 K under 1 mPa for 5 h before the measurement.

Results and discussion

In order to clarify the effect of Si/Al ratio on the hydophile–hydrophobe balance of zeolites, water adsorption isotherms were measured on faujasite samples with various Si/Al ratios and shown in Fig. 1. Water adsorption onto Na-$Y_{5.5}$ with low Si/Al ratio is extremely high, and H_2O molecules fill approximately 72% of the micropore volume calculated based on N_2 adsorption measurement. The adsorption isotherm of Na-$Y_{5.5}$ is of Langmuir type rising sharply in the low relative pressure region, indicating that Na-$Y_{5.5}$ is highly hydrophilic. In contrast, zeolite samples with high Si/Al ratios, such as Na-Y_{42} and Na-Y_{344}, exhibit lower adsorption performance. The higher the Si/Al ratio, the lower the water adsorption. Na-Y_{344} with the highest Si/Al ratio shows extremely low water adsorption, indicating its high hydrophobicity. As the Si/Al ratio increases, rise of the adsorption isotherm in the low relative pressure region becomes slower, showing that zeolite micropore surface changes from hydrophilicity to hydrophobicity. This behavior resembles the water adsorption behavior of faujasite zeolite which was described in our last report [29]. However, unlike H-Y_{770} with still higher Si/Al ratio, Na-Y_{344} showed no increase in adsorption in the high relative pressure region. Such increase observed with H-Y_{770} is presumably due to the following reason: since H-Y_{770} underwent hydrothermal and acid treatments for dealuminization, hydroxyl groups were formed in a large amount on the secondary micropore surface generated as the result of structural destruction [36]. The above-mentioned result

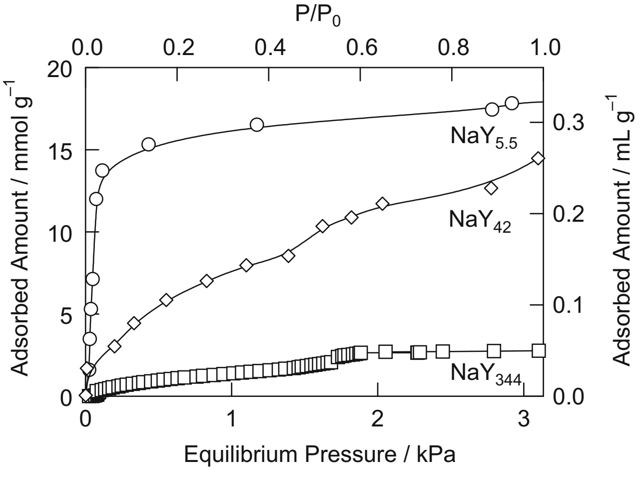

Fig. 1 Adsorption isotherms of water on faujasites

with Na-Y_{344} also closely resembles the water adsorption behavior of highly silicious ZSM-5 [39].

Figure 2 shows chloroform adsorption isotherms of faujasite samples with various Si/Al ratios, and Fig. 3 shows curves representing differential heats of adsorption of each sample. Referring to Fig. 2, the adsorption isotherm of any faujasite zeolite is of Langmuir type in which a steep rise is typically observed in the low pressure region, implying high adsorptive interaction between chloroform molecules and faujasite micropore surface. Chloroform adsorption on Na-Y_{344} is lower than that on Na-$Y_{5.5}$, presumably due to blocked micropore and destroyed zeolite framework structure which were caused by dealuminization treatment. This result is consistent with the actual micropore volume reduction that occurs in N_2 adsorption measurement. Referring to the differential heat of adsorption curves, the initial heat of adsorption is slightly higher for Na-$Y_{5.5}$ with low Si/Al ratio (high Al content) than for Na-Y_{344}. This indicates that a specific interaction takes place between the electrostatic field of zeolite micropore surface and the dipole of chloroform molecules. As adsorption progresses, heats of adsorption increase indicating that chloroform adsorption is affected more by the interaction between adsorbed molecules than by the interaction between electrostatic field and dipole. These results coincide well with those reported by Mellot et al. [21] When adsorption progresses further into the later stage in which almost all zeolite micropores are filled up with adsorbates, differential heats of adsorption begin to decrease, ultimately approaching 29.4 kJ mol^{-1}, the heat of liquefaction of chloroform.

Figure 4 shows chloroform adsorption isotherms of ZSM-5 samples with various Si/Al ratios, and Fig. 5 shows curves representing differential heats of adsorption. The adsorption isotherm of any ZSM-5 sample is also of Langmuir type, rising sharply in the low pressure region.

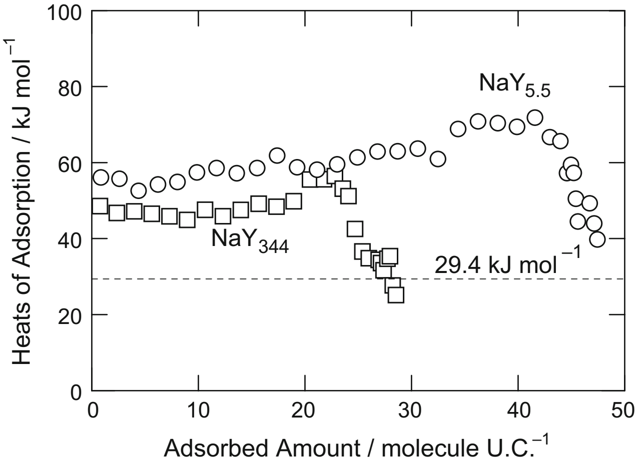

Fig. 3 Differential heats of adsorption of chloroform on faujasites at 303 K

Unlike the case in Fig. 1 or the case of water adsorption on ZSM-5 [39], chloroform adsorption does not decrease with an increase in Si/Al ratio. Adsorption amount was almost constant at about 1.5 mmol g^{-1}, forming adsorption isotherms of almost the same shape. This indicates that chloroform gas adsorption onto zeolite is dominated by dispersive interaction. As shown in Fig. 5, the initial heats of adsorption on ZSM-5-25Na and ZSM-5-70Na with rather low Si/Al ratios (high Al contents) are higher than those on ZSM-5-200Na and ZSM-5-1000Na with low Al contents, supposedly due to a specific interaction between the electrostatic field of ZSM-5 micropore surface and the dipole of chloroform molecules. Unlike the case with faujasite, differential heats of adsorption on ZSM-5 show no increase as adsorption progresses. This is presumably because multi-molecular-layer adsorption does not occur in ZSM-5 due to its small pore diameter.

Figures 6 and 7 show adsorption isotherms and differential heats of adsorption of chloroform on mordenite

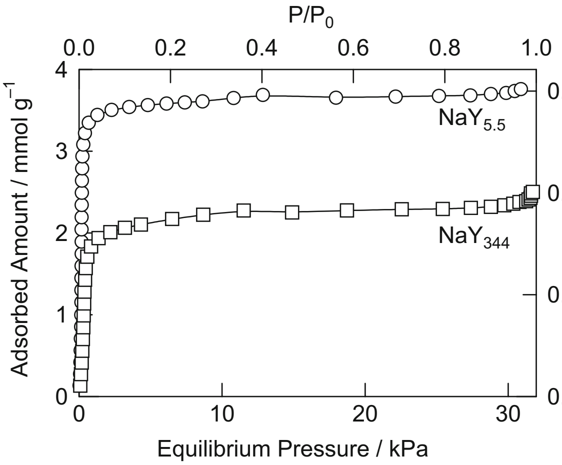

Fig. 2 Adsorption isotherms of chloroform on faujasites at 303 K

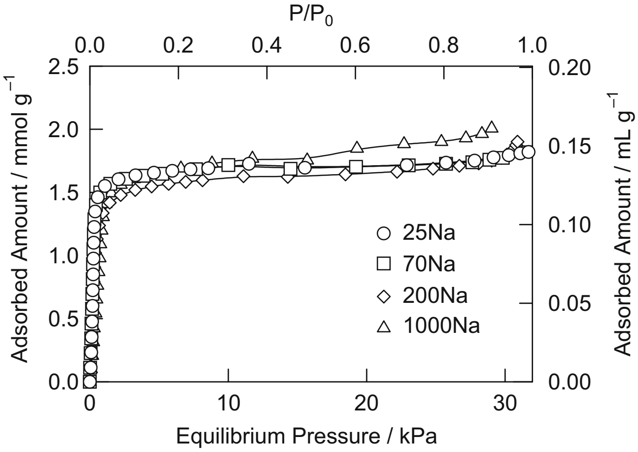

Fig. 4 Adsorption isotherms of chloroform on ZSM-5 at 303 K

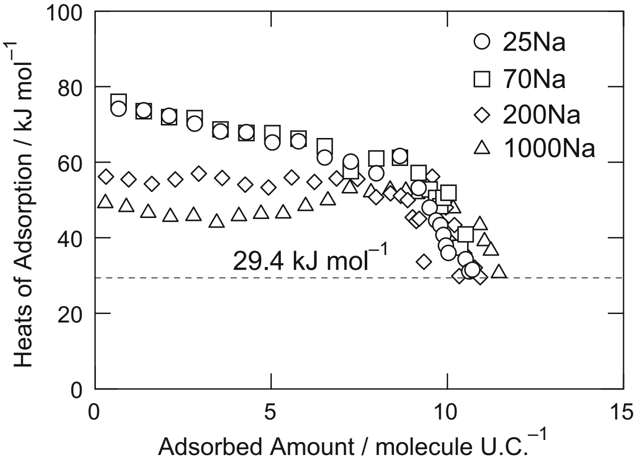

Fig. 5 Differential heats of adsorption of chloroform on ZSM-5 at 303 K

samples with various Si/Al ratios. Saturated amount of adsorption is high in M-20 with low Al, which is similar to the finding that the adsorption of benzene molecule was enhanced with a decrease in the number of Al (i.e., Na^+ ion) [40]. This can be explained by considering that benzene or chloroform adsorption occurs only in main channel of mordenites and is sterically hindered by the presence of Na ion in the channel. Like ZSM-5 samples, the initial heat of adsorption of mordenites also changes with the Si/Al ratio. Of all types of zeolite, M-10 sample exhibits the highest initial heat of adsorption at about 90 kJ mol^{-1}, most likely due to the following two reasons. First, since the Al content ratio (Al/(Si+Al)) of M-10 framework is rather high among zeolites used in the present study, M-10 provides high electrostatic field strength on the micropore surface. Second, the micropore diameter of the main channel of M-10 is small at about 0.67 to 0.70 nm, compared to about 0.74 to 1.3 nm of faujasite samples. This small micropore diameter results in the overlapping effect on the adsorption potential of micropore wall [41].

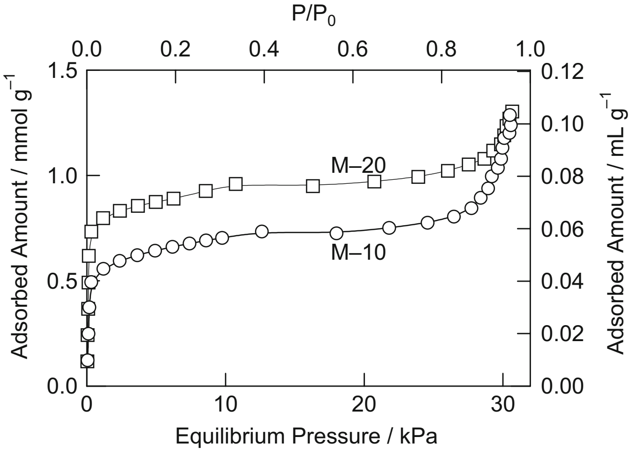

Fig. 6 Adsorption isotherms of chloroform on mordenite at 303 K

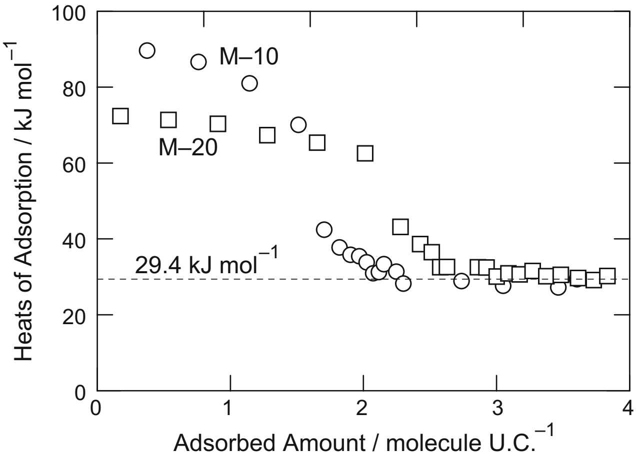

Fig. 7 Differential heats of adsorption of chloroform on mordenite at 303 K

Since adsorption behavior of zeolite changes with Si/Al ratio in the extremely low relative pressure region as shown in Figs. 2, 4, and 6, the relationship between Al content of zeolite framework and Langmuir constant "*a*" representing adsorption affinity was analyzed and is shown in Fig. 8. In cases of faujasites and ZSM-5, the constant "*a*" increases linearly with Al content with a large slope in the region [Al/(Si+Al)]<0.02 and with a small slope in the region [Al/(Si+Al)]>0.02. This phenomenon reflects that the electrostatic field strength of zeolite micropore surfaces influences the affinity of zeolites to chloroform molecules whatever the extent is. Therefore, the initial stage of chloroform adsorption on zeolites is dominated by the interaction between the electrostatic field of zeolite micropore surface and the dipole of chloroform molecules. Zeolites with low Si/Al ratio (high Al content in framework) provides high adsorptive interaction. A small slope in Al-rich region may be explained as follows; since the zeolitic pore volume is

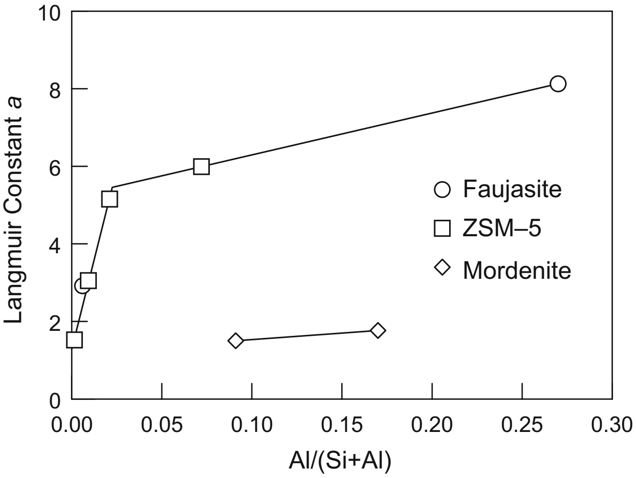

Fig. 8 A relationship between Al content of zeolite framework and Langmuir constant "*a*"

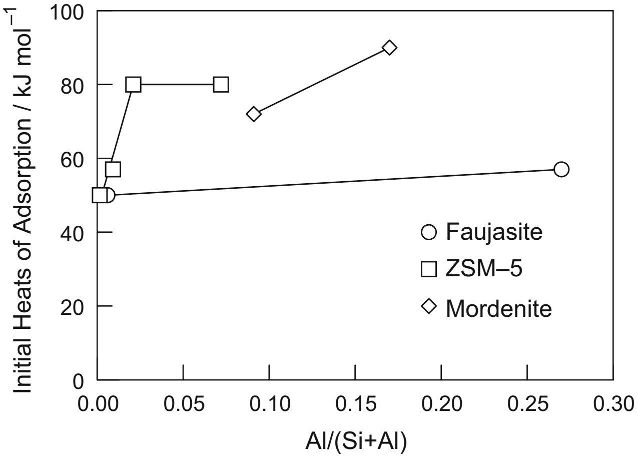

Fig. 9 A relationship between Al content of zeolite framework and the initial heat of adsorption

limited, a part of active site neighboring to Al atom is difficult to interact specifically with chloroform molecule due to steric hindrance. This is analogous with the relationship between heats of immersion of water and Al content of faujasites with various Si/Al ratio [28]. In case of mordenites, only a slight dependence was observed between Al content and the constant "*a*." Itabashi et al. reported that only 2.7 Na^+ ions among eight per unit cell exist in the main channel in M-10 and no Na ion in the main channel in M-20 [40]. Furthermore, as mentioned above, chloroform adsorption occurs only in the main channel and is sterically hindered by Na^+ ions. Therefore, the effect of the presence of Al (i.e., Na^+ ion) on the adsorption affinity may be small in case of mordenites.

Figure 9 shows the relationship between the Al content of framework and the initial heat of adsorption of each zeolite sample. For any type of zeolite, as the Al content of framework increases, the initial heat of adsorption increases temporarily. The rate of increase is the highest with ZSM-5.

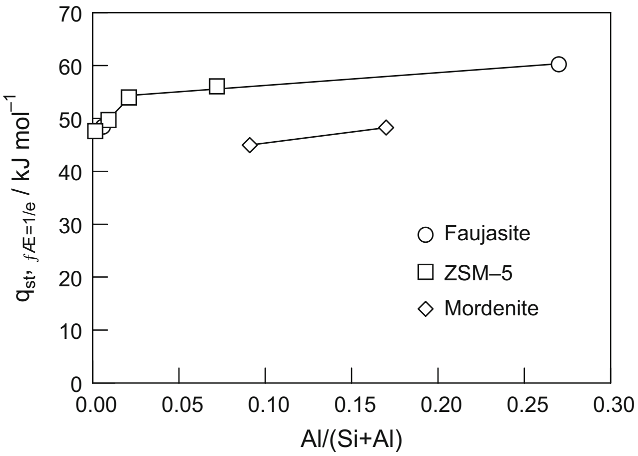

Fig. 10 A relationship between Al content of zeolite framework and isosteric heat of adsorption

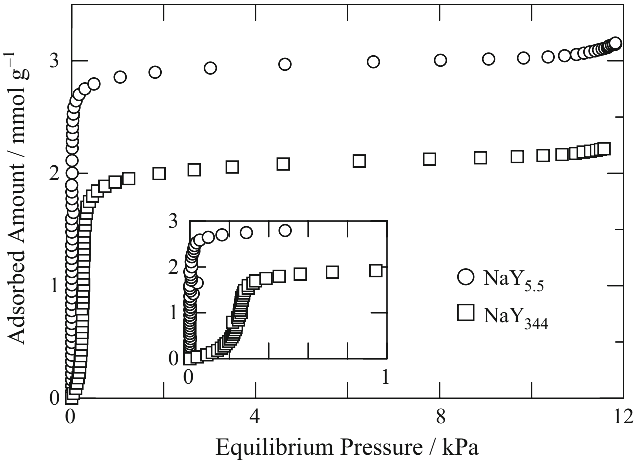

Fig. 11 Adsorption isotherms of trichloroethylene (TCE) on faujasites at 303 K

For all types of zeolite (faujasite, ZSM-5, and mordenite), samples with lower Si/Al ratio (higher Al content) provide higher initial heat of adsorption. This tendency is the most prominent with ZSM-5. Specifically, difference in the initial heat of adsorption between ZSM-5-1000Na and ZSM-5-25Na is approximately 30 kJ mol^{-1}. For mordenite samples, difference between the highest and lowest values for initial heat of adsorption is approximately 5 kJ mol^{-1}. For faujasite samples, this difference is about 7 kJ mol^{-1}. The micropore diameter of ZSM-5 samples ranges from about 0.51 to 0.55 nm, that of mordenite samples from about 0.67 to 0.70 nm, and that of faujasite samples from about 0.74 to 1.3 nm. Obviously, there is a certain correlation between the initial heat of adsorption and the micropore diameter of zeolite.

The ZSM-5 micropore diameter is extremely close to the chloroform molecule diameter which ranges from about 0.46 to 0.64 nm. This causes superposition effect on the adsorption potential of micropore wall [41]. As the result, ZSM-5 is

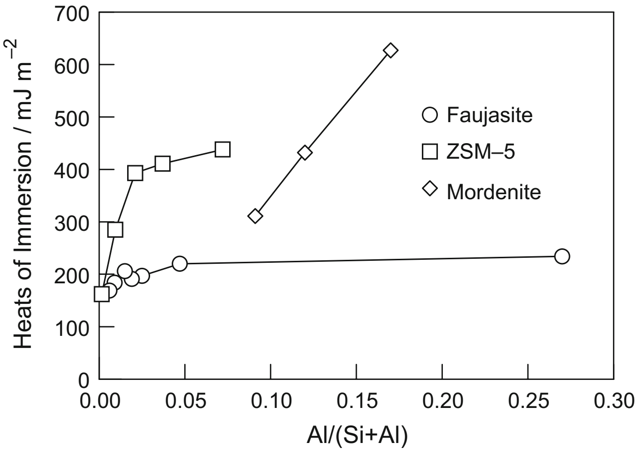

Fig. 12 Dependence of heats of immersion of zeolites into chloroform

influenced largely by interaction between the electrostatic field of zeolite micropore surface and the dipole of chloroform molecules, and the initial heat of adsorption of ZSM-5 differs largely depending on the Si/Al ratio.

It is well known that Dubinin–Radushkevich equation gives values of the micropore volume and βE_0 by use of the adsorption isotherm [42]. β and E_0 refer to affinity coefficient and characteristic adsorption energy, respectively. The isosteric heat of adsorption, q_{st}, at the adsorption amount, $1/e$ times the saturated amount, can be calculated by using Eq. 1,

$$q_{\mathrm{st}} = H_{\mathrm{v}} + \beta\, E_0 \tag{1}$$

where H_{v} is the heat of vaporization [43]. Figure 10 shows the relationship between the thus calculated isosteric heat of adsorption and Al content of framework.

Like the case of Langmuir constant "*a*" as shown in Fig. 8, the equivalent heat of adsorption also has a temporary correlation with the Al content of zeolite framework, which confirms that interaction between the electrostatic field of zeolite micropore surface and the dipole of chloroform molecules increases with the Al content of framework. However, the equivalent heat of adsorption increases only from 40 to 45 kJ mol^{-1}, implying little influence by the Al content. This confirms that chloroform adsorption to zeolite micropores is governed by the London dispersion force, with little influence by the interaction between electrostatic field and dipole. This result is consistent with the finding that immersion heat of zeolite in chloroform changes little with the Al content of framework [28].

Measurements were also made of trichloroethylene adsorption onto faujasite samples with various Si/Al ratios for comparison with the chloroform adsorption behavior. Figure 11 shows the adsorption isotherms.

Saturated adsorption of trichloroethylene is almost the same as that of chloroform (see Fig. 2), except that saturated adsorption changes with Si/Al ratio in the low-pressure region of adsorption isotherm, as shown in Fig. 11. Since trichloroethylene molecules provide unsaturated bonding, they have larger peculiar interaction with the electrostatic field of zeolite micropore surface than do chloroform molecules. Therefore, Na-Y_{344} with high Si/Al ratio produces a weak electrostatic field on the micropore surface, resulting in lower initial adsorption than that to Na-$\mathrm{Y}_{5.5}$.

The relationship between Al content of zeolite framework and heat of immersion into chloroform is shown in Fig. 12. The tendencies of heat of immersion are similar to the results of the initial heat of adsorption. In case of ZSM-5, the heat of immersion increases linearly with Al content with a large slope in the region [Al/(Si+Al)]<0.02 and are almost constant (about 420 mJ m^{-1}) in the [Al/(Si+Al)] above 0.02. In case of mordenite, the heat of immersion increases linearly with Al content with a large slope. In case of faujasite, the heat of immersion increases with Al content with a small slope in the small [Al/(Si+Al)] region, then became almost constant with a value of about 230 mJ m^{-2}, which value is about half of the value of ZSM-5. The value of heat of immersion of M-10 is about 630 mJ m^{-2}, which value is the highest among all samples. This tendency was also observed in the results of initial heats of adsorption.

Conclusion

For all types of zeolite, the chloroform adsorption isotherm is of Langmuir type in shape. Chloroform molecules fill almost all zeolite micropores, with the saturated adsorption depending only on the zeolite micropore volume, not on the micropore structure or the Si/Al ratio.

However, for all types of zeolite, the initial heat of adsorption, calculated from the measurements of differential heat of adsorption, and the heat of immersion are higher for zeolite with lower Si/Al ratio (i.e., higher Al content in framework). This tendency is prominent particularly with ZSM-5 whose micropore diameter is almost equal to the chloroform molecule diameter, due to the superposition effect on the adsorption potential of micropore wall.

The above-mentioned results have led us to the following conclusion. Chloroform adsorption onto zeolite micropores is governed, in its early stage, by the peculiar interaction between the electrostatic field of zeolite micropore surface and the dipole of chloroform molecules, and in its later stage, by the London dispersion force. The adsorption continues until zeolite micropores have been filled up almost completely with chloroform molecules.

References

1. Leonard AJ, Eric BS, Thomas SF (1985) Am Ind Hyg Assoc J 46:20
2. Urano K (1986) Kagaku Kogaku 50:180
3. Thomas EB, Yoram C (1990) Ind Eng Chem Res 29:1338
4. Suzuki Y, Koizumi A, Takeuchi Y (1993) Kagaku Kogaku Ronbunshu 19:381
5. Nakai T, Ziyang L, Satoh Y, Katoh Y (1994) Nippon Kagaku Kaishi:371
6. Oda H, Nishimoto T, Kishima T (1997) Tanso 176:20
7. James EK, Wigton A (1999) Environ Sci Technol 33:250
8. Miyake Y, Sakoda A, Yamanashi H, Kaneda H, Suzuki M (2003) Water Res 37:1852
9. Wang GS, Jae WL, Hee M (2003) J Chem Eng Data 48:286
10. Krasnova TA, Kirsanov MP, Ushakova OI (2001) Russ J Phys Chem 75:1753
11. Kubota K, Nishitani R, Sakamoto M, Imakoma H (2004) J Chem Eng Japan 37:483
12. Kawazoe K, Sakoda A (1986) Kagaku Kogaku 50:182
13. Sakoda A, Kawazoe K, Suzuki M (1987) Water Res 21:717
14. Tanaka E, Naitoh R, Sakata Y, Kasaoka S (1988) Nippon Kagaku Kaishi:1549

15. Sakata Y, Muto A, Azhar U, Nishino H (1996) Kemikaru Enjiniyaringu 41:29
16. Uchida M, Ito S, Kawasaki N, Nakamura T, Tanada S (1999) J Colloid Interface Sci 220:406
17. Deepak SP, Kiran VA, Howard LG, Chester AV (1995) AIChE Symp Ser 91:1
18. Prashant SC, Howard LG (1997) Appl Catal B 14:37
19. Chandak MV, Lin YS (1998) Environ Technol 19:941
20. Bouvier F, Weber G (1998) J Therm Anal Calorim 54:881
21. Mellot CF, Cheetham AK, Harms S, Savitz S, Gorte RJ, Myers AL (1998) Langmuir 14(23):6728–6733
22. Caroline FM, Anthony KC, Shani H, Scott S, Raymond JG, Alan LM (1998) J Am Chem Soc 120:5788
23. Manuel SS, Teresa B, Fernando R (1999) Phys Chem Chem Phys 1:4529
24. Hernandez MA, Gonzalez AI, Rojas F, Asomoza M, Solis S, Portillo R (2007) Ind Eng Chem Res 46:3373
25. Kawai T, Tsutsumi K (1992) Colloid Polym Sci 270:711
26. Kawai T, Tsutsumi K (1994) Colloid Polym Sci 272:830
27. Kawai T, Tsutsumi K (1995) Colloid Polym Sci 273:787
28. Kawai T, Yanagihara T, Tsutsumi K (1994) Colloid Polym Sci 272:1620
29. Tsutsumi K, Kawai T, Yanagihara T (1994) Studies in Surface Science and Catalysis vol.83, Zeolites and microporous crystals: 217
30. Nakahara K, Ida T, Arima Y, Sato G (1992) Extended Abstract 9th Int Zeolite Conf: RP175
31. Shirahama Y, Ida T, Arima Y (1993) Japan Patent 5-97427
32. Beyer HK, Belenykaja I (1980) Stud Surf Sci Catal 5:203
33. Beyer HK, Belenykaja I, Ferenc H (1985) J Chem Soc Faraday Trans I 81:2889
34. Sulikowski B, Borbely G, Beyer HK, Karge HG, Mishin IW (1989) J Phys Chem 93:3240
35. Kawai T, Tsutsumi K (1998) Adsorption 4:225
36. Kawai T, Tsutsumi K (1999) J Colloid Interface Sci 212:310
37. Tsutsumi K, Koh HQ, Hagiwara S, Takahashi H (1975) Bull Chem Soc Jpn 48:3576
38. Masuda T, Taniguchi H, Tsutsumi K, Takahashi H (1978) Bull Chem Soc Jpn 51:633
39. Tsutsumi K, Mizoe K (1989) Colloids Surf 37:29
40. Itabashi K, Fukushima T, Igawa K (1986) Zeolites 6:30
41. Matsumoto A, Zhao J, Tsutsumi K (1997) Langmuir 13:496
42. Dubinin MM (1960) Chem Rev 60:235
43. Kaneko K (1994) J Membr Sci 96:59